J. Fluid Mech. (2004), *vol.* 521, *pp.* 105–114.
DOI: 10.1017/S0022112004001739 Printed in the United Kingdom

A bound on mixing efficiency for the advection–diffusion equation

By JEAN-LUC THIFFEAULT[1], CHARLES R. DOERING[2] AND JOHN D. GIBBON[1]

[1]Department of Mathematics, Imperial College London, SW7 2AZ, UK

[2]Department of Mathematics and Michigan Center for Theoretical Physics, University of Michigan, Ann Arbor, MI 48109-1109, USA

(Received 3 August 2004 and in revised form 3 September 2004)

An upper bound on the mixing efficiency is derived for a passive scalar under the influence of advection and diffusion with a body source. For a given stirring velocity field, the mixing efficiency is measured in terms of an *equivalent diffusivity*, which is the molecular diffusivity that would be required to achieve the same level of fluctuations in the scalar concentration in the absence of stirring, for the same source distribution. The bound on the equivalent diffusivity depends only on the functional 'shape' of both the source and the advecting field. Direct numerical simulations performed for a simple advecting flow to test the bounds are reported.

1. Introduction

In this work we apply some recent developments in the analysis of the Navier–Stokes equations (Doering & Foias 2002) to mixing and the advection–diffusion equation. Mixing phenomena are ubiquitous with applications in atmospheric science, oceanography, chemical engineering, and microfluidics, to name a few. Here we focus on the generic problem of the advection–diffusion equation with a source that replenishes the variance of the passive scalar. The stirring is effected by a specified velocity field, which may or may not be turbulent. Our analysis of an idealized model lends mathematical precision and rigour to conventional scaling arguments often invoked for these kinds of problems.

For the passive scalar, complicated behaviour – and efficient mixing – is often observed even for laminar velocity fields. This is the well-known effect of chaotic advection (Aref 1984; Ottino 1989). Thus we can choose the stirring (the advecting velocity field) to be any divergence-free, possibly time-dependent flow field. The mixing efficiency then depends on specific properties of the stirring field as well as the manner in which the scalar concentration is injected, which is exactly what would be expected. The bound on mixing efficiency derived in this paper has that feature: it depends on the stirring field and the source distribution. This is very helpful as it allows comparison of the relative effectiveness of various stirring scenarios for, say, a specified source. The bounds we obtain are also valid for turbulent flows, as we make no assumptions about the smoothness of the stirring field. A recent study by Schumacher, Sreenivasan & Yeung (2003) has produced bounds on the derivative moments of the concentration field; here we shall focus on the undifferentiated quadratic moment. As will become evident, the methods of this paper can also be extended to produce bounds on derivatives of the concentration field.

2. System description

The advection–diffusion equation for the concentration $\theta(\boldsymbol{x}, t)$ of a passive scalar is

$$\partial_t \theta + \boldsymbol{u} \cdot \nabla \theta = \kappa \, \Delta \theta + s, \tag{2.1}$$

where κ is the molecular diffusivity and $s(\boldsymbol{x}, t)$ is a source function with zero spatial mean. The domain we consider is a periodic box of side L, i.e. $\boldsymbol{x} \in \mathbb{T}^d$, the d-dimensional torus. The velocity field $\boldsymbol{u}(\boldsymbol{x}, t)$ could be obtained by solving Navier–Stokes or some other set of equations, but here we shall simply consider it to be an arbitrary L^2 divergence-free vector field. Hence without loss of generality we may take the solution $\theta(\boldsymbol{x}, t)$ to be spatially mean zero at all times.

Variations in the source term in (2.1) maintain the inhomogeneity of the concentration field. The stirring term may lead to the formation of sharp gradients of concentration that then enhance the effect of molecular diffusion. For definiteness we assume that both the source and the stirring act on a comparable scale, $\ell \leqslant L$. Because of periodicity, L/ℓ is an integer. We introduce these two distinct scales in order to be able to consider the infinite volume limit, $L \to \infty$ at fixed ℓ, for the final results.

We shall use the fluctuations in the concentration as a useful measure of the degree of well-mixedness, as has long been the practice (e.g. Danckwerts 1952; Edwards, Sherman & Breidenthal 1985; Rehab *et al.* 2000). To characterize the fluctuations in θ, we use the variance,

$$\Theta^2 := \langle L^{-d} \, \|\theta\|^2_{L^2(\mathbb{T}^d)} \rangle, \tag{2.2}$$

of the spatially mean-zero concentration. The angle brackets $\langle \cdot \rangle$ denote a long-time average, which we will assume exists for the quantities of interest, and $\|\cdot\|_{L^2(\mathbb{T}^d)}$ is the L^2 norm on $\mathbb{T}^d$. As control parameters we use the variance of the source and a measure of the kinetic energy density of the stirring field,

$$S^2 := \langle L^{-d} \, \|s\|^2_{L^2(\mathbb{T}^d)} \rangle, \quad U^2 := \langle L^{-d} \, \|\boldsymbol{u}\|^2_{L^2(\mathbb{T}^d)} \rangle. \tag{2.3}$$

Thus, Θ, S, and U are spatio-temporal averages respectively of fluctuations in the scalar concentration $\theta(\boldsymbol{x}, t)$, the source $s(\boldsymbol{x}, t)$, and the fluid velocity $\boldsymbol{u}(\boldsymbol{x}, t)$. An efficient mixing configuration would have small Θ for a given S and U, indicating a steady state with small variations in the concentration. In general we expect that increasing U at fixed S should decrease Θ, for this represents more vigorous stirring, while increasing S at fixed U should augment Θ. We will show in this paper that Θ has a lower bound proportional to $S\ell/U$, so that a source with large fluctuations necessarily produces a poorly mixed state unless U is increased sufficiently.

In order to keep track of the effects of the amplitudes of the source variation and stirring intensity and their characteristic length scales independently from the influence of the particular 'shapes' of the input and mixing functions, we decompose s and $\boldsymbol{u}$ into the dimensional amplitudes (S and U) and dimensionless shape functions (Φ and $\boldsymbol{\Upsilon}$) according to

$$s(\boldsymbol{x}, t) = S \, \Phi(\boldsymbol{x}/\ell, t/\tau), \quad \langle L^{-d} \, \|\Phi\|^2_{L^2(\mathbb{T}^d)} \rangle = 1, \tag{2.4}$$

$$\boldsymbol{u}(\boldsymbol{x}, t) = U \, \boldsymbol{\Upsilon}(\boldsymbol{x}/\ell, t/\tau), \quad \langle L^{-d} \, \|\boldsymbol{\Upsilon}\|^2_{L^2(\mathbb{T}^d)} \rangle = 1, \tag{2.5}$$

where τ is an appropriate time scale characterizing the source and stirring. Of course either or both may be time-independent, but in any case we presume periodicity or statistical stationarity with identifiable periods or relaxation times.

3. The bounds

Now consider an arbitrary smooth (dimensionless) spatially periodic function $\Psi(\boldsymbol{x}/\ell, t/\tau)$ normalized such that

$$\left\langle L^{-d} \int_{\mathbb{T}^d} \Psi(\boldsymbol{x}/\ell, t/\tau)\, \Phi(\boldsymbol{x}/\ell, t/\tau)\, \mathrm{d}^d x \right\rangle = 1. \tag{3.1}$$

For example because of the normalization in (2.4), $\Psi = \Phi$ could be a possible choice if it is sufficiently smooth. Multiply (2.1) by Ψ and space–time average. Using (2.4) and (3.1) and integrating by parts, we may express S as

$$S = -\left\langle L^{-d} \int_{\mathbb{T}^d} (\partial_t \Psi + \boldsymbol{u}\cdot\nabla\Psi + \kappa\, \Delta\Psi)\, \theta\, \mathrm{d}^d x \right\rangle. \tag{3.2}$$

Note that the operator acting on Ψ in (3.2) is the adjoint of the advection–diffusion operator, which suggests how the method can be generalized to other linear operators with a body source (e.g. the magnetic induction operator of dynamo theory (Childress & Gilbert 1995)).

The Cauchy–Schwartz inequality implies the bound

$$S \leqslant \langle L^{-d} \| \partial_t \Psi + \boldsymbol{u}\cdot\nabla\Psi + \kappa\, \Delta\Psi \|^2_{L^2(\mathbb{T}^d)} \rangle^{1/2} \Theta. \tag{3.3}$$

Then substituting the scaled variables $T = t/\tau$ and $\boldsymbol{y} = \boldsymbol{x}/\ell$ and using (2.5), we have

$$S \leqslant \frac{U\Theta}{\ell} \langle \| \Omega \|^2_{L^2(\mathbb{I}^d)} \rangle^{1/2} \tag{3.4}$$

where $\mathbb{I} = [0, 1]$ is the unit torus and

$$\Omega(\boldsymbol{y}, T) := -Sr\, \partial_T \Psi(\boldsymbol{y}, T) - \boldsymbol{\Upsilon}(\boldsymbol{y}, T)\cdot\nabla_y \Psi(\boldsymbol{y}, T) + \frac{1}{Pe}\, (-\Delta_y \Psi(\boldsymbol{y}, T)). \tag{3.5}$$

Here the Péclet number is $Pe = U\ell/\kappa$. If the velocity field is time-dependent with time scale τ, the dimensionless number $Sr := \ell/U\tau$ may be regarded as a Strouhal number; in any case, we shall refer to it as the Strouhal number even if the time scale τ is unrelated to $\boldsymbol{u}$.

In principle inequality (3.4) could be sharpened by varying Ψ to provide as tight a bound as possible, as performed by Doering, Eckhart & Schumacher (2003) for the power consumption rate in the Navier–Stokes equations. We will not pursue that direction here; rather we will produce explicit limits via simple estimates.

Applying the Minkowski inequality to (3.4), we see that

$$S \leqslant \frac{U\Theta}{\ell} (c_1 + Pe^{-1}\, c_2) \tag{3.6}$$

where

$$c_1 := \langle \| Sr\, \partial_T \Psi + \boldsymbol{\Upsilon}\cdot\nabla_y \Psi \|^2_{L^2(\mathbb{I}^d)} \rangle^{1/2}, \tag{3.7a}$$

$$c_2 := \langle \| \Delta_y \Psi \|^2_{L^2(\mathbb{I}^d)} \rangle^{1/2}, \tag{3.7b}$$

are dimensionless constants, independent of Pe and Θ. The constant c_1 depends on dimensional quantities only through the Strouhal number; it also depends explicitly on the stirring shape-function $\boldsymbol{\Upsilon}$. Note also that the function Ψ depends indirectly on the source shape-function Φ through its normalization (3.1), so that both the source and stirring shapes enter the bound. The constant c_2 controls the diffusive part while κ only enters through the Péclet number in (3.6). We still have the freedom to

choose Ψ to optimize c_1 for a particular problem, that is, for particular source and stirring shapes Φ and $\boldsymbol{\Upsilon}$.

For small Pe, we can focus on the c_2 term in (3.6) and obtain the bound $S \leqslant c_2 \Theta \kappa / \ell^2$. As we increase the source amplitude S, holding the other parameters constant, the time-averaged variance Θ^2 must eventually increase. An increase in the variance implies that the scalar is more poorly mixed. There is no avoiding this unless we increase κ or decrease the scale of the source ℓ: the efficiency of mixing is intrinsically related to the diffusive mixing rate on the scale of the source variance injection, i.e. κ/ℓ^2.

For large Pe, the more interesting limit for many physical problems, we focus on the c_1 term in (3.6) to get the bound $S \leqslant c_1 U \Theta / \ell$. (This is true for sufficiently smooth Ψ.) As we increase the source amplitude S, holding everything else constant, the bound (3.6) again implies that we must eventually see an increase in the steady-state variance, Θ^2. However, unlike the small-Pe case, we can now (potentially) postpone that increase by raising U, i.e. by stirring more vigorously. The exact value of c_1 depends on both shape-functions, but (3.7a), where c_1 is defined, can be broken up by the Minkowski and Hölder inequalities to give

$$c_1 \leqslant Sr \langle \, \| \partial_T \Psi \|^2_{L^2(\mathbb{T}^d)} \, \rangle^{1/2} + \sup_{\boldsymbol{y},t} |\nabla_{\boldsymbol{y}} \Psi| , \tag{3.8}$$

which is uniform in the shape of the stirring. The large-Pe bound has the nice feature of being independent of the diffusivity κ, a result expected to hold for the passive scalar under turbulent or chaotic mixing. However, the linear scaling with U in (3.6) is not always appropriate, as will be seen in § 5 for the specific case we have studied numerically. Note also that the bound (3.8) on c_1 still involves the velocity for time-dependent Ψ through the Strouhal number. If it is possible to choose Ψ to be time-independent and still satisfy the normalization condition (3.1) – for example if the source s is time-independent – then we have the bound

$$c_1 \leqslant \sup_{\boldsymbol{y}} |\nabla_{\boldsymbol{y}} \Psi| , \tag{3.9}$$

which is satisfied for all possible stirring flows (i.e. any shape function $\boldsymbol{\Upsilon}$) independently of U.

We can also derive a lower bound for S. The average variance dissipation rate, ϵ, satisfies

$$\epsilon = \langle \kappa \, L^{-d} \, \| \nabla \theta \|^2_{L^2(\mathbb{T}^d)} \, \rangle = \left\langle L^{-d} \int_{\mathbb{T}^d} s(\cdot, \boldsymbol{x}) \, \theta(\cdot, \boldsymbol{x}) \, \mathrm{d}^d x \right\rangle \tag{3.10}$$

where we have used the fact that $\| \theta \|_{L^2(\mathbb{T}^d)}$ is uniformly bounded in time, which is true under the physical assumption that $\| s \|_{L^2(\mathbb{T}^d)}$ is itself uniformly bounded in time. By using Poincaré's inequality in (3.10) we have $(\epsilon/\kappa)^{1/2} \geqslant (2\pi\Theta)/L$, and the Cauchy–Schwartz inequality along with the normalization of Φ in (2.4) gives $\epsilon \leqslant S \, \Theta$. Together these give the bound

$$S \geqslant (2\pi/L)^2 \, \kappa \, \Theta . \tag{3.11}$$

This lower bound reflects that no matter how we stir – or if we do not stir – there is still some diffusive dissipation of the scalar variance. The lower bound (3.11) also implies that if there is any variance Θ^2 present at the steady state, then it must be due to some minimum amount of amplitude of the source; stirring alone can never generate scalar variance in this kind of model.

The consequence of the two bounds for S is that larger Θ must eventually imply large S (from (3.11), at fixed κ and L), but large S does not necessarily imply large Θ, as the difference can be made up by a large U in (3.6). This is what makes enhanced mixing possible.

We may also estimate the typical size of small scales in the scalar field. Using the bound $S \geqslant \epsilon/\Theta$ mentioned above, we can transform (3.4) and (3.6) into upper bounds for ϵ, namely

$$\left(\frac{2\pi}{L}\right)^2 \kappa\, \Theta^2 \leqslant \epsilon \leqslant \frac{U\Theta^2}{\ell}(c_1 + Pe^{-1}\, c_2), \tag{3.12}$$

where the lower bound is obtained via Poincaré's inequality. If we define a scalar dissipation scale λ,

$$\lambda^{-2} \coloneqq \frac{\langle \|\nabla\theta\|^2_{L^2(\mathbb{T}^d)} \rangle}{\langle \|\theta\|^2_{L^2(\mathbb{T}^d)} \rangle} = \frac{\epsilon}{\kappa\, \Theta^2} \tag{3.13}$$

(the Batchelor scale (Batchelor 1959), an analogue of the Taylor microscale for the Navier–Stokes equations) then

$$L/(2\pi) \geqslant \lambda \geqslant \ell\,(c_1\, Pe + c_2)^{-1/2}\,. \tag{3.14}$$

For large Pe, the smallest possible size of this dissipation scale is proportional to $Pe^{-1/2}$, a standard theoretical estimate (Childress & Gilbert 1995).

4. Mixing efficiency and equivalent diffusivity

As a physically meaningful measure of mixing efficiency, we define the *equivalent diffusivity*†

$$\kappa_{\mathrm{eq}} \coloneqq \beta\, \frac{S\ell^2}{\Theta} \leqslant \bar{c}_1\, U\ell + \bar{c}_2\, \kappa. \tag{4.1}$$

The factor β is the norm of the solution of the purely diffusive problem,

$$\beta \coloneqq \|(Sr\, Pe\, \partial_T + \Delta_{\boldsymbol{y}})^{-1}\Phi\|_{L^2(\mathbb{I}^d)}, \tag{4.2}$$

and the constants $\bar{c}_1$ and $\bar{c}_2$ are respectively c_1 and c_2 multiplied by β. The extra factor of β ensures that $\kappa_{\mathrm{eq}} = \kappa$ for $U = 0$, which is the purely diffusive case. This corresponds to the choice $\Psi = (Sr\, Pe\, \partial_T + \Delta_{\boldsymbol{y}})^{-2}\Phi/\beta$, for which $\bar{c}_2 = 1$. Note that $(Sr\, Pe\, \partial_T + \Delta_{\boldsymbol{y}})^{-N}$ is defined in the Galerkin sense on the Fourier expansion of Φ.

The equivalent diffusivity κ_{eq} compares the source amplitude (S) to the steady-state fluctuations in the concentration field (Θ); as its name implies, it may be regarded as the molecular diffusivity needed to give a comparable amount of mixing in the absence of flow. A high-Péclet-number steady-state mixing device should operate with as high an equivalent diffusivity as possible compared to the molecular diffusivity. Alternatively, we may interpret the ratio $\kappa^2_{\mathrm{eq}}/\kappa^2$ as the supression factor for the solution's variance. That is, if θ_0 is the solution of the diffusion equation with the

† We refrain from calling κ_{eq} an 'effective' diffusivity because this already carries a definition in the literature (e.g. Young 1999). There the effective diffusivity is defined in terms of a large-scale gradient in the concentration, whereas here we use the amplitude of the source, which makes more sense in the present context. The relationship between that traditional effective diffusivity κ_{eff} and κ_{eq} is $\kappa_{\mathrm{eq}} = \kappa_{\mathrm{eff}}\,(\Theta/G\ell)^2$, where G is a linear gradient of concentration (Schumacher *et al.* 2003). Other notions of effective diffusivity are also used in the context of anomalous diffusion (e.g. Isichenko 1992) and turbulence (e.g. Pope 2000).

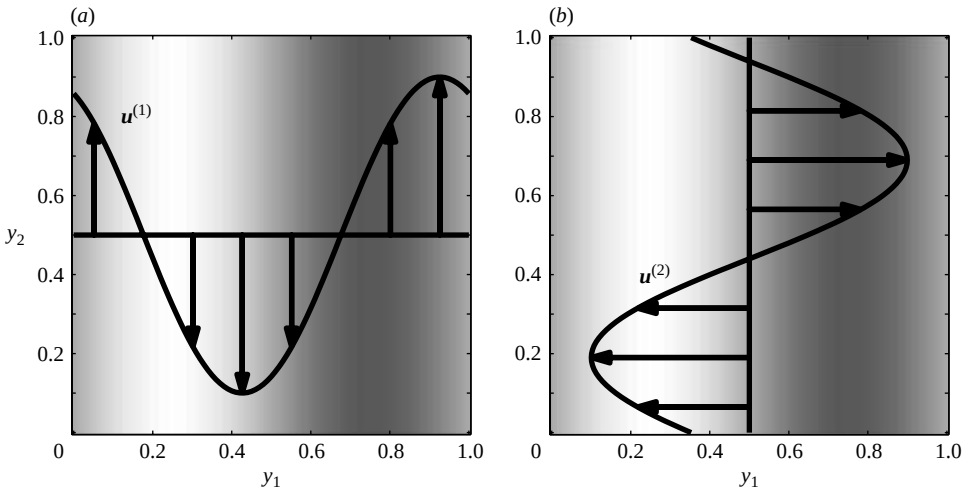

FIGURE 1. The sine flow (5.1) for (*a*) the first half and (*b*) the second half of each period, represented here with random phases χ_1 and χ_2. The velocity field alternates direction, but the source distribution (as represented by the shaded background) is stationary.

same source but no stirring and Θ_0^2 is its variance, then the definition (4.1) is simply $\kappa_{\rm eq}^2/\kappa^2 = \Theta_0^2/\Theta^2$.

In the regime of small U, the variance is proportional to the amplitude of the source, a response we expect when the stirring does not play an important role. A large equivalent diffusivity means that we are obtaining a well-mixed distribution (small Θ) compared to the initial inhomogeneity in the source (S); as explained in § 3, for fixed κ and ℓ this can only be achieved by increasing U.

The equivalent diffusivity can also be bounded from below by using (3.11),

$$\kappa_{\rm eq} \geqslant \kappa\, \beta\, (2\pi\, \ell/L)^2\,. \tag{4.3}$$

The worst lower bound for the mixing efficiency would be achieved by injecting scalar variance at scale ℓ while stirring to keep the dominant scale of the concentration fluctuation field as L.

5. Bounds for the sine flow

As an example application, we consider the well-studied two-dimensional Zeldovich sine flow, or random wave flow (Pierrehumbert 1994; Antonsen *et al.* 1996). This flow consists of alternating horizontal and vertical sine shear flows, with phase angles χ_1 and $\chi_2 \in [0, 2\pi]$ randomly chosen at each time period, τ (see figure 1). In the first half of the period, the velocity field is

$$\boldsymbol{u}^{(1)}(\boldsymbol{x}, t) = \sqrt{2}\, U(0,\ \sin(2\pi x_1/L + \chi_1)); \tag{5.1a}$$

and in the second half-period it is

$$\boldsymbol{u}^{(2)}(\boldsymbol{x}, t) = \sqrt{2}\, U(\sin(2\pi x_2/L + \chi_2), 0). \tag{5.1b}$$

The flow is incompressible, and U is defined consistently with (2.3), so that $\boldsymbol{\Upsilon}$ is read off from (5.1) by dropping U and replacing $\boldsymbol{x}/L$ by $\boldsymbol{y}$. As a source function, we choose $s(\boldsymbol{x}) = \sqrt{2}\, S\, \sin(2\pi x_1/L)$, from which $\Phi(\boldsymbol{y}) = \sqrt{2}\, \sin(2\pi y_1)$. Here the source and stirring scale length ℓ is equal to the system size L. The purely diffusive solution with

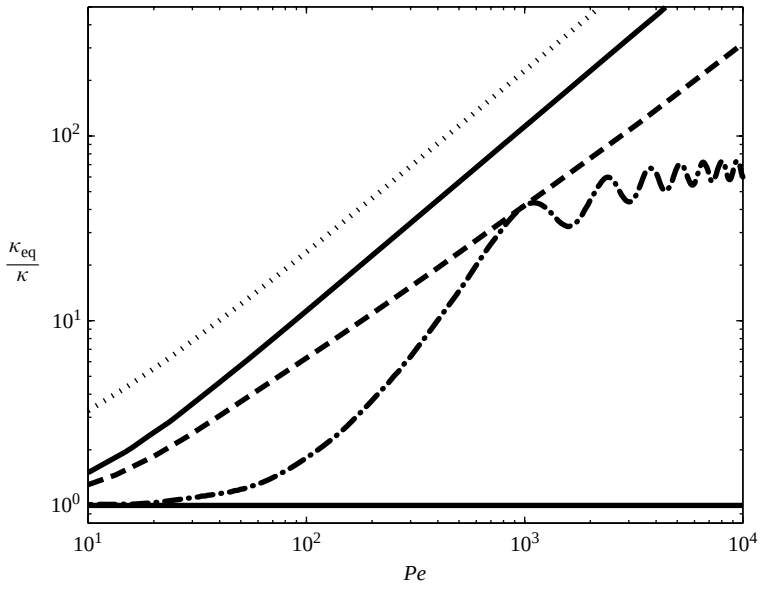

FIGURE 2. Ratio of equivalent diffusivity κ_{eq} to molecular diffusivity κ for the sine flow (5.1). The upper solid line is the upper bound (5.3) and the lower bound (4.3) is shown as a horizontal solid line. The upper limit (3.9) indicated by the dotted line is valid for any stirring flow with this source distribution. The dashed line is the result of direct numerical simulations with U and τ fixed (i.e. with constant $Sr = 1$). The dashed-dot curve plots simulation data with κ and τ held constant while varying U (in this case $Sr = Pe^{-1}$).

this source distribution gives $\beta = 1/(2\pi)^2$ in (4.2), and hence the lower bound $\kappa_{eq} \geqslant \kappa$ for the equivalent diffusivity.

The challenge now lies in choosing Ψ to optimize the bound as best we can. The simplest choice is to take $\Psi = \Phi$, as this automatically satisfies the normalization (3.1). Inserting that form into (3.7) (with $\partial_T \Psi = 0$), we find $c_1 = \sqrt{2}\,\pi$ and $c_2 = (2\pi)^2$, for a bound on the equivalent diffusivity

$$\frac{\kappa_{eq}}{\kappa} \leqslant \frac{Pe}{2\sqrt{2}\pi} + 1. \tag{5.2}$$

We can get a tighter bound by using (3.4), which does not use the Minkowski inequality, and exploiting the statistical isotropy and homogeneity of the flow:

$$\frac{\kappa_{eq}}{\kappa} \leqslant \sqrt{\frac{Pe^2}{8\pi^2} + 1}. \tag{5.3}$$

The bound (5.3) is optimal over time-independent Ψ for our choice of stirring and source shape functions. Because $\boldsymbol{\Upsilon}$ is discontinuous in time (which is not an obstacle to the bounding procedure), this particular velocity field does not yield a form of Ω that is easily optimized over time-dependent Ψ. So for this example with a steady source and a time-independent multiplier Ψ, our bound is uniform in the Strouhal number Sr.

Figure 2 shows the upper and lower bounds together with the results of direct numerical simulations of the advection–diffusion equation (2.1) with this single-mode source and the sine flow (5.1). The upper and lower bounds (5.3) and (4.3) are plotted as solid lines.

There are various ways of varying Pe in this model. For one, we can hold U and τ fixed (both at the value 1) and vary κ, in which case the Strouhal number is fixed. The dashed line in figure 2 is the result of the simulation with $Sr = 1$ (in all simulations reported here, $\ell = L = 1$). We see that the bound qualitatively captures the behaviour of the equivalent diffusivity in this case, although we do not have a wide enough high-Pe range to determine if the high-Pe asymptotic scaling agrees with the bounds.

Another simulation strategy is to hold κ and τ fixed (in this case at 10^{-3} and 1, respectively) and vary U. The data from this simulation with $Sr = Pe^{-1}$ are plotted as the dash-dot line in figure 2. We observe that this method of stirring is less effective at suppressing variance in the concentration at any value of $Pe \neq 10^3$ where all the parameters coincide. In particular, with this stirring the enhancement of the equivalent diffusivity tends to saturate rather than increase indefinitely at high Pe. This can be understood as a 'resonance' effect of the periodic boundary conditions: as U increases at fixed τ and the typical displacement $U\tau$ exceeds ℓ, the velocity field merely maps the concentration fluctuations onto periodic copies of themselves rather than mixing them up within each periodic cell. Because the bound in (5.3) is uniform in τ, it should be compared at a given value of Pe to the largest possible equivalent diffusivity achievable by any τ, which can only improve the agreement with the bound. These different simulation schemes illustrate the importance of the Strouhal number for the mixing efficiency and, not unexpectedly, highlight the need for further analysis to extract the Strouhal number dependence of the best bounds.

The dotted line in figure 2 is a weaker upper bound obtained from (3.9) using $\Psi = \Phi$; it sets an absolute limit on the mixing efficiency achievable with any stirring field shape at any Strouhal number for this particular source distribution.

Finally, we note that there are flow fields at arbitrarily high values of Pe and arbitrary Sr that saturate the lower bound $\kappa_{\mathrm{eq}}/\kappa = 1$ for this source shape. Indeed, any flow field $\boldsymbol{u}$ with no x_2 dependence (and arbitrary x_1 and t dependence) simply moves the scalar along iso-concentration lines to no effect whatsoever. This simple example is a particular case of a more general result concerning the existence of 'ineffective' stirring fields (W. R. Young 2004, personal communication) – essentially integrable fields without chaos.

6. Conclusions

It is encouraging that the equivalent diffusivities in figure 2 rise away from the diffusive lower bound as Pe increases, indicating that there is hope of more nearly saturating the upper bound with more complex flows. From the example of the sine flow, it is clear that in general there is a non-trivial Sr dependence, even for steady sources, that warrants further investigation. Unlike the solution of the full problem which requires a non-zero diffusivity to keep Θ uniformly bounded in time, the bounding procedure does not require any diffusivity. That is, for large Pe we may neglect c_2 from the bound altogether and focus on c_1 to try and minimize it with respect to Ψ. Of course, the resulting optimal bound on $\kappa_{\mathrm{eq}}/U\ell$ may still depend in a complicated way on Pe and Sr for specific stirring and source distributions.

The high-Pe scaling of the bound obtained in this paper might be related to an analogous one in combustion theory (Constantin *et al.* 2000). There it was found that the bulk burning rate V can satisfy an 'optimal linear enhancement bound', $V \geqslant KU$, where K is a constant and U is the magnitude of the advecting field. The type of flow required for linear enhancement, called 'percolating flows' in Constantin *et al.* (2000), connects distant regions of unburned material. Perhaps these flows also

produce linear asymptotic scaling with Pe for the equivalent diffusivity enhancement, but we have not yet investigated this.

Although we specified a body source in our problem with periodic conditions, a source of concentration at impenetrable boundaries can be mimicked by a sharp source concentrated near the walls (Balmforth & Young 2003). However, the type of wall boundary condition that can be modelled in this manner is restricted to fixed scalar flux.

In closing we note that all of our analysis, as well as the general result that $\kappa_{\rm eq}/\kappa \coloneqq \beta S\ell^2/\kappa\Theta \leqslant \bar{c}_1 Pe + \bar{c}_2$, depend on the source distribution being smooth enough to have a finite variance S^2. Point sources, for example where $s \sim \delta(\boldsymbol{x})$, may be of interest in applications but do not have finite variance. In this situation we may still define the mixing efficiency and an equivalent diffusivity via $\kappa_{\rm eq}/\kappa \coloneqq \Theta_0/\Theta$ where Θ^2 and Θ_0^2 are the scalar variances with and without the stirring; these scalar variances are finite even for δ-like sources in two and three spatial dimensions. However, the anticipated behaviour suggested by the consideration of smooth sources, i.e. that the equivalent diffusivity enhancement $\kappa_{\rm eq}/\kappa$ and/or its upper bound could be $\sim Pe$, may not be realized with more singular sources. The investigation of those models is left for future work.

We thank P. Constantin, K. R. Sreenivasan, and W. R. Young for helpful comments. J.-L. T. and C. R. D. are grateful for the hospitality of the 2002 Summer Program in Geophysical Fluid Dynamics at the Woods Hole Oceanographic Institution, where this work was initiated. C. R. D. was supported in part by NSF Awards PHY9900635 and PHY0244859.

REFERENCES

Antonsen, Jr., T. M., Fan, Z., Ott, E. & Garcia-Lopez, E. 1996 The role of chaotic orbits in the determination of power spectra. *Phys. Fluids* **8**, 3094–3104.

Aref, H. 1984 Stirring by chaotic advection. *J. Fluid Mech.* **143**, 1–21.

Balmforth, N. J. & Young, W. R. 2003 Diffusion-limited scalar cascades. *J. Fluid Mech.* **482**, 91–100.

Batchelor, G. K. 1959 Small-scale variation of convected quantities like temperature in turbulent fluid. *J. Fluid Mech.* **5**, 113–133.

Childress, S. & Gilbert, A. D. 1995 *Stretch, Twist, Fold: The Fast Dynamo*. Springer.

Constantin, P., Kiselev, A., Oberman, A. & Ryzhik, L. 2000 Bulk burning rate in passive–reactive diffusion. *Arch. Rat. Mech. Anal.* **154**, 53–91.

Danckwerts, P. V. 1952 The definition and measurement of some characteristics of mixtures. *Appl. Sci. Res.* A **3**, 279–296.

Doering, C. R., Eckhart, B. & Schumacher, J. 2003 Energy dissipation in body-forced plane shear flow. *J. Fluid Mech.* **494**, 275–284.

Doering, C. R. & Foias, C. 2002 Energy dissipation in body-forced turbulence. *J. Fluid Mech.* **467**, 289–306.

Edwards, A. C., Sherman, W. D. & Breidenthal, R. E. 1985 Turbulent mixing in tubes with transverse injection. *AIChE J.* **31**, 516.

Isichenko, M. B. 1992 Percolation, statistical topography, and transport in random-media. *Rev. Mod. Phys.* **64**, 961–1043.

Ottino, J. M. 1989 *The Kinematics of Mixing: Stretching, Chaos, and Transport*. Cambridge University Press.

Pierrehumbert, R. T. 1994 Tracer microstructure in the large-eddy dominated regime. *Chaos Soitons Fractals* **4**, 1091–1110.

Pope, S. B. 2000 *Turbulent Flows*. Cambridge University Press.

Rehab, H., Antonia, R. A., Djenidi, L. & Mi, J. 2000 Characteristics of fluorescein dye and temperature fluctuations in a turbulent near-wake. *Exps. Fluids* **28**, 462–470.

Schumacher, J., Sreenivasan, K. R. & Yeung, P. K. 2003 Schmidt number dependence of derivative moments for quasi-static straining motions. *J. Fluid Mech.* **479**, 221–230.

Young, W. R. 1999 *Stirring and Mixing: Proc. 1999 Summer Program in Geophysical Fluid Dynamics* (ed. J.-L. Thiffeault & C. Pasquero). Woods Hole Oceanographic Institution, Woods Hole, MA, USA. http://gfd.whoi.edu/proceedings/1999/PDFvol1999.html